Supporting Information

Poly(ferrocenylsilane) Electrolytes as Gold Nanoparticle Foundry: "Two-in-One" Redox Synthesis and Electrosteric Stabilization, and Sensing Applications

Song Jing,[1] Yen Nee Tan,[1*] Dominik Jańczewski,[2] Mark Hempenius,[3] Jian Wei Xu,[1*] Hui Ru Tan,[1] Julius G. Vancso[3*]

[1]Institute of Material Research and Engineering, A*STAR (Agency for Science, Technology and Research), 2 Fusionpolis Way, Innovis, #08-03, Singapore 138634.

[2]Laboratory of Technological Processes, Faculty of Chemistry, Warsaw University of Technology Noakowskiego 3, 00-664 Warsaw, Poland.

[3]MESA+ Institute for Nanotechnology, Materials Science and Technology of Polymers, University of Twente, P.O. Box 217, 7500 AE Enschede, the Netherlands.
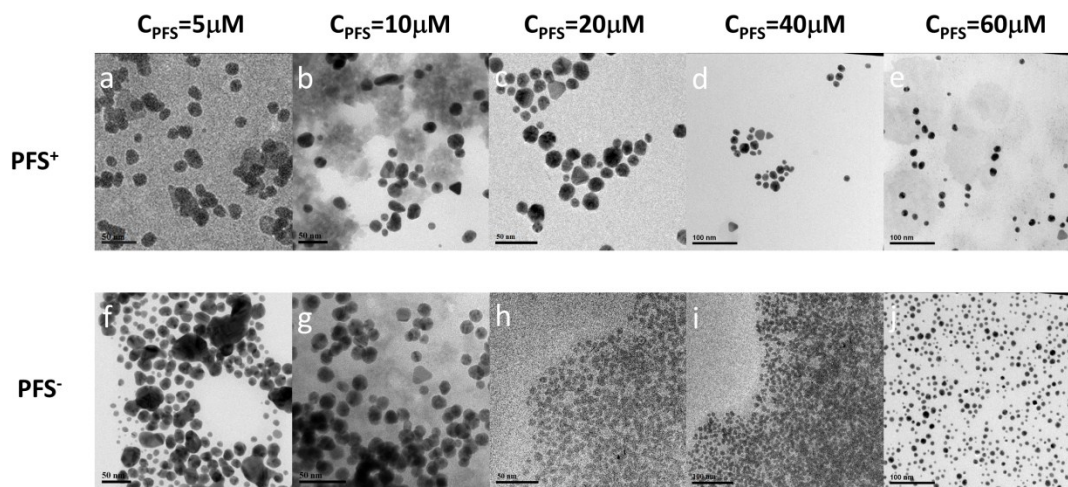
AFM images of PFS@AuNPs

The morphology and size of AuNPs were investigated by atomic force microscopy (AFM). Figure S1 shows the morphology and phase images of PFS$^{+/-}$@AuNPs, respectively. The particles were well dispersed on mica surfaces. The lateral dimensions of AuNPs obtained are in the range of 80nm~120nm (PFS$^+$@AuNPs) and 40nm~80nm (PFS$^-$@AuNPs) which were much larger than the results obtained from TEM images. The main reason for this AFM inherent feature, profile broadening, is the tip convolution which is due to the finite radius of AFM tips.[1] The height of the AuNPs are 10nm~14nm for (PFS$^+$@AuNPs) and 4nm~10nm (PFS$^-$@AuNPs) which is consistent with the mean size of the particles measured by TEM. Figure S1b and S1d show phase images of AuNPs which refer to recording the phase shift signal in tapping mode AFM. The phase shift or phase lag can be related local energy dissipation by

tip-sample interaction. For the hybrid AuNPs, inorganic gold particles are elastic and the protection layer, i.e. PFS polyelectrolytes, are viscoelastic, leading to large phase shifts. (The same AFM tip was used for the experiments.) In the phase image of PFS$^-$@AuNPs, the bright area can be related to the gold nanoparticles while the obvious dark peripheral regions are attributed to the capping polymer layer. For PFS$^+$@AuNPs, no contrast of phase image was observed on the hybrid particles. This may be due to the thin protection layer on the particles.
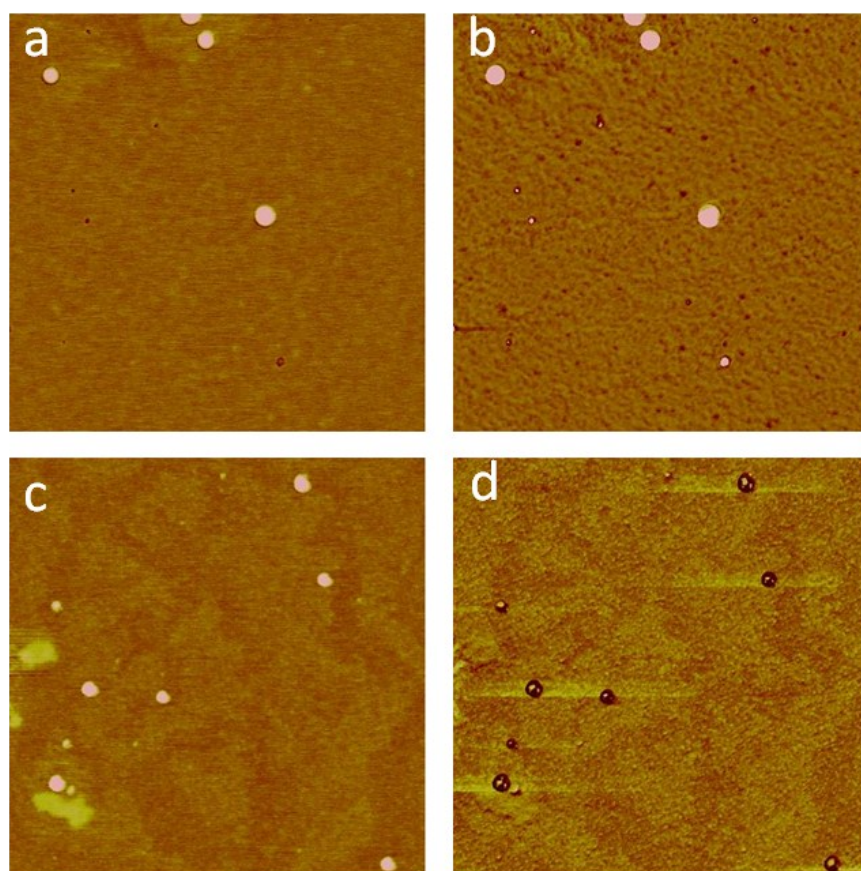
Figure S1. AFM images of AuNPs a) height image b) phase image of PFS$^+$@AuNPs c) height image d) phase image of PFS$^-$@AuNPs, [PFS$^{+/-}$]:[HAuCl$_4$]= 60μM:1mM.

TEM images of PFS@AuNPs

Figure S2. TEM images of AuNPs of different sizes prepared by controlling the concentration of polyelectrolytes while keeping C_{HAuCl4} = 1mM. The concentration of PFS$^+$ is a) 5μM, b) 10μM, c) 20μM, d) 40μM, e) 60μM The concentration of PFS$^-$ is f) 5μM, g) 10μM, h) 20μM, i) 40μM, j) 60μM.

pH effect on PFS$^-$@AuNPs stability

PFS$^-$@AuNPs were dispersed at various pH in water. Figure S3a shows the normalized UV-Vis spectra obtained on these systems. No obvious change was observed. The particles are stable in the solution for the pH range from 2 to 10.

At pH =2 solution, upon mixing with FeCl$_3$, an immediate red shift of UV-Vis spectra of the particles was observed. After subsequently mixing with Vit C, a blue shift of the UV/Vis spectra was detected. However, in pH=10 solution, after subsequently adding FeCl$_3$ and Vit C, the particles did not show the assembly- disassembly behavior. This may be because the oxidant FeCl$_3$ is a pH sensitive agent. At higher pH, FeCl$_3$ is not efficient to oxidize ferrocene to ferrocenium.
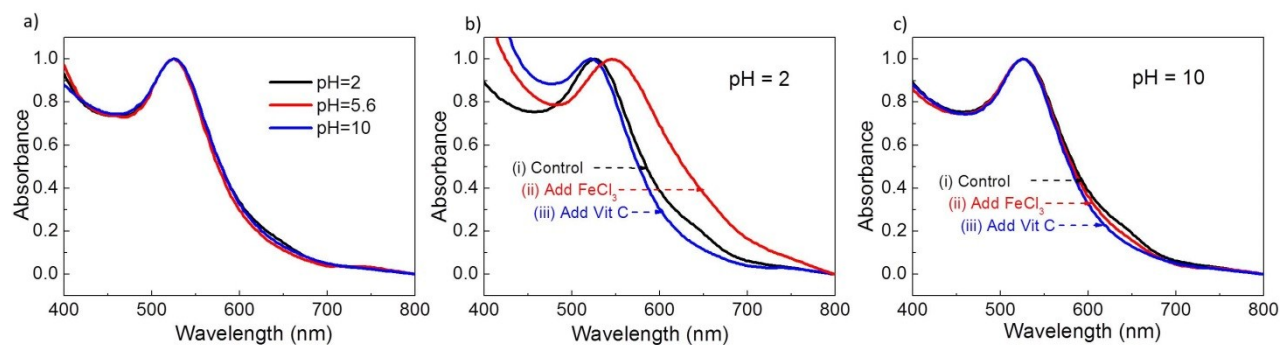
Figure S3. Normalized UV-Vis spectra of PFS⁻@AuNPs a) at various pH b) at pH=2 upon subsequently adding FeCl$_3$ and Vit C c) at pH=10 upon subsequently adding FeCl$_3$ and Vit C.

## Temperature effect on PFS⁻@AuNPs stability

The PFS⁻@AuNPs solution was heated in water bath at a temperature 60°C for 15 min. The UV-Vis spectrum of the particle is identical to the unheated particle solution (Shown in Figure S4).
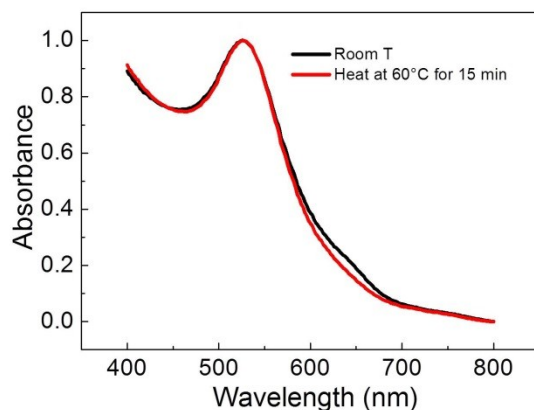
Figure S4. Normalized UV-Vis spectra of PFS⁻@AuNPs at different temperature.

## Other bio-substance interference effects on PFS⁻@AuNPs stability

We also studied the salt effect on aggregation. Results show that PFS⁻@AuNPs are stable in up to 3M NaCl solution. In addition, we also studied some bio-substance effects such as a) an amino acid, L-Lysine; b) a monosaccharide, galactose; and c) an enzyme, Horseradish Peroxidase. In Figure S5, the particle mixing with 3 different bio-substances shows similar assembly-disassembly behavior upon subsequently adding FeCl$_3$ and Vit C.
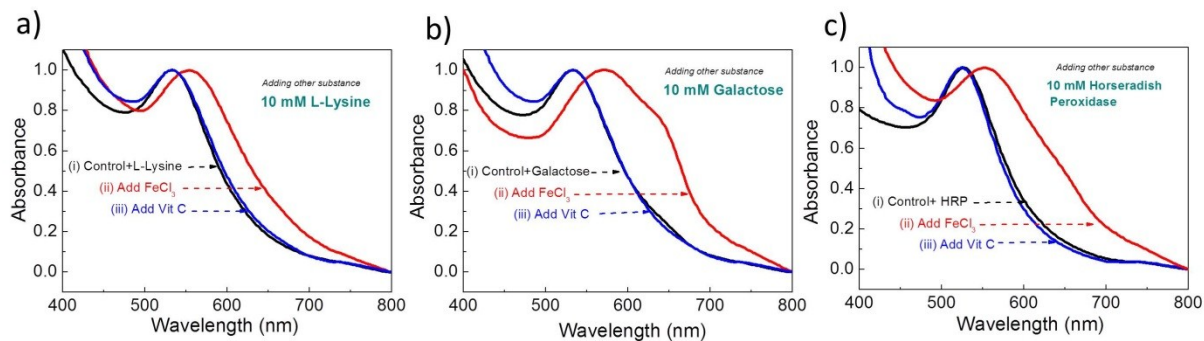
Figure S5. Normalized UV-Vis spectra of PFS⁻@AuNPs with bio-substances upon subsequently adding $FeCl_3$ and Vit C.

Other reducing reagents detected by PFS⁻@AuNPs

PFS⁻@AuNPs was used as a colorimetric probe to detect model redox molecules, Vit C. In principle, other redox molecules which can either oxidize the ferrocene units or reduce the ferrocenium units of PFS main chain may induce similar particle assembly-disassembly behavior. To prove this concept, we also tried three other reducing agents for comparison.
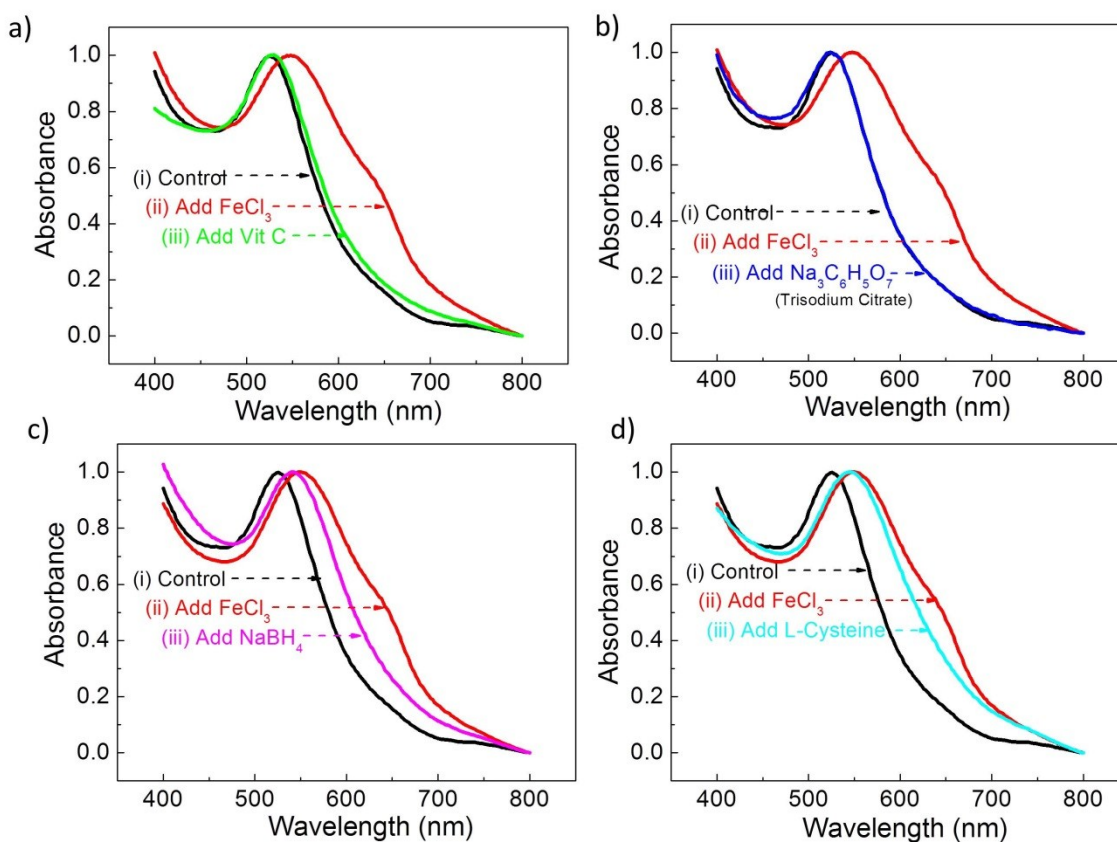
Figure S6. Normalized UV-Vis spectra of PFSox⁻@AuNPs adding with various reducing agents a) Vit C; b) Trisodium Citrate; c) NaBH₄ d) L-Cysteine.

Figure S6 a-d shows red-shift in the UV-Vis spectra of PSF⁻@AuNPs (as control solution) upon mixing with 0.5mM of $FeCl_3$ accompanied by an immediate color change of the nanoparticle solution from red to purple. In contrast, the blue shift in the UV-Vis spectra of particles is observed after adding 1mM reducing agents. The absorbance ratio values obtained at two wavelengths (A_{650}/A_{530}) was used to quantify the degree of aggregation, ψ.

$\psi_{\text{original PFS-@AuNPs}}$ **(0.157)** $=\psi_{\text{Trisodium Citrate}}$ **(0.157)** $< \psi_{\text{VitC}}$ **(0.1856)** $< \psi_{\text{NaBH4}}$ **(0.268)** $< \psi_{\text{L-Cystine}}$ **(0.34)** $< \psi_{\text{PFS}^-\text{oxAuNPs}}$ **(0.5104)**

This result shows that different reducing agents have different capacities to change the degree of particle aggregation. Trisodium Citrate and Vit C are good reducing agents for ferrocenium. The aggregated oxidized particles are re-dispersed in the solution upon mixing with them. However, the

aggregated oxidized particles are not fully re-dispersed after adding the other two reducing agents (NaBH$_4$ is effective for the reduction of aldehydes and ketones to alcohols and L-Cysteine is a monothiol reducing agent).

References

1.   N. G. Orji, H. Itoh, C. Wang and R. G. Dixson, *Instrumentation, Metrology, and Standards for Nanomanufacturing, Optics, and Semiconductors Viii*, 2014, **9173**.